PERGAMON

International Journal of Heat and Mass Transfer 45 (2002) 4151–4161

International Journal of HEAT and MASS TRANSFER

www.elsevier.com/locate/ijhmt

Theoretical model for the thermal conductivity of a packed bed of solid spheroids in the presence of a static gas, with no adjustable parameters except at low pressure and temperature

A.J. Slavin *, V. Arcas, C.A. Greenhalgh, E.R. Irvine, D.B. Marshall

Department of Physics, Trent University, Peterborough ON, Canada K9J 7B8

Received 21 September 2001; received in revised form 10 March 2002

Abstract

Many analytical models exist for the thermal conductivity of packed pebble beds in a static gas, but all require adjustable parameters to give good fits to experimental data. The present paper differs from earlier ones in including a measurable parameter for the particle roughness. With this, the conductivity for an uncompressed bed can be calculated with no adjustable parameters, provided the conductance of the solid is much greater than that of the gas and gas pressures are above about 4 kPa. Agreement with experimental data is typically within 15% over a wide range of temperature and pressure.

1. Introduction

The thermal conductivity of packed pebble beds in a static gas is of interest in a number of applications. Such beds have been proposed for thermal insulation [1,2] and as the breeder blanket about a fusion reactor [3], and are also of interest as beds for chemical reactions [4] and in drying processes [5]. The cost of making accurate measurements on test beds is high in both time and apparatus, so considerable effort has gone into developing models which can be used predictively to improve bed performance.

An exact analytical expression for the bed conductivity is not possible even for an idealized, perfectly regular packing of the spheres because the conductivity varies spatially in a complex fashion with temperature and pressure, and has different dependencies for the solid, gas, and radiative contributions. As a result, existing models are of two basic types. The first is the finite-element numerical model which can treat the three-dimensionality of the problem by dividing the bed into a great many cells with the temperature and heat flow matched at their boundaries, but it can be difficult to extract the relative importance of different conduction pathways from such computer models. The second type is the analytical model which breaks the problem into a relatively few distinct conduction paths (the contact between pebbles, the gas between them, radiation, etc.) and calculates the overall bed conductance as a series/parallel combination of the individual conductances for these paths. To make such models mathematically tractable, one normally treats the heat flow as being in straight lines within and between the spheres. The advantage to the analytical model, if successful, is that it enables one to evaluate easily the relative contributions of each pathway as a function of temperature, gas pressure, and particle size and roughness, and use this in the bed design. The appropriateness of the assumptions and approximations used in either type of model must be evaluated, in the end, from the agreement between the theoretical predictions and actual experimental data. If the agreement is good for beds of several different materials, gases, and particle sizes and roughnesses, then

* Corresponding author. Tel.: +1-705-748-1011 Ext. 1289; fax: +1-705-748-1652.

E-mail address: aslavin@trentu.ca (A.J. Slavin).

0017-9310/02/$ - see front matter
PII: S0017-9310(02)00117-5

Nomenclature

A_{cp}	base area of the close-packed unit cell
A_v	base area of the void cell
a	accommodation coefficient
B	average gap radius in the SLH model
C_v	heat capacity per molecule
D	molecular diameter
g_{av}	average gap width in the SLH model
G	total conductance of the unit cell
G_c	conductance though the contact points between contiguous spheroids
G_{cp}	conductance of the close-packed region of the unit cell
G_i	gas conductance through the "inner" region between spheres where $2/3\lambda >$ gap
G_o	gas conductance through the "outer" gap between spheres where $2/3\lambda <$ gap
G_{gv}	gas conductance across the void region
G_r	conductance between spheres by radiation
G_{rv}	conductance by radiation across the void region
G_s	conductance through the solid sphere
G_v	conductance of the void region of the unit cell
h_r	average height of the short-range surface roughness
j	temperature jump distance at a surface
k	Boltzmann's constant
K	effective thermal conductivity of the packed bed
K_i	gas conductivity in the "inner" region where $2/3\lambda >$ gap
K_o	gas conductivity in the "outer" region where $2/3\lambda <$ gap
K_s	conductivity of the bulk solid
l	gap between two surfaces confining the gas
l_o	any convenient estimate for the average length for the heat flow
L	height of the unit cell
n	molecular number density ($n = P/kT$)
N_c	number of effective contact points per sphere
p	packing fraction
P	gas pressure
Pr	Prandtl number
$\dot{Q}$	heat flow in watts through the unit cell
R	average radius of a spheroid
T	temperature in Kelvins
$\overline{v}$	molecular velocity
V	volume of the unit cell

Greek symbols

α_c, α_i, α_r, α_s	geometrical correction factor for the conductances G_c, G_i, G_r and G_s, respectively
γ	$\gamma = (C_v + k/2)/C_v$
δ	area of direct contact between adjacent spheroids
ϵ	thermal emissivity
σ_S	Stefan–Boltzmann constant
λ	molecular mean free path
θ	polar angle
θ_{max}	maximum polar angle of integration when calculating G_o
θ_λ	polar angle at which $2/3\lambda = 2h_r$
τ	$\tau = (h_r + j)/R$

one has some confidence in using the model predictively in other situations.

This paper considers an analytical model. In most beds of interest, the conductance of a single solid particle is much greater than for other contributions: radiation, conduction through the gas, or conduction across the direct contact between spheres. Therefore, the bed conductivity is limited by the latter three mechanisms. At very low gas pressure and temperature, the contact conductance will dominate; it must always be obtained experimentally, since there is no way of estimating the contact area from first principles, at least in an uncompressed bed. At sufficiently high temperature, the radiation term will be important. However, it has long been recognized that, for the majority of practical cases, the gaseous conduction in the vicinity of the points of contact between pebbles (where the gap is least) is the dominant conduction path [6]. Attempts to incorporate such gaps into a model generally fall into two categories: (a) those relating the gap width to the bed packing density (e.g., the model of Zehner et al. [6] referred to as ZBS) and (b) those using a value for surface roughness as a measure of the minimum gap (e.g., in Ref. [6], for the wall-to-particle heat transfer). However, attempts to describe experimental data by models of the first type often require unrealistically large values of the particle–particle contact area (treated as a fitting parameter) to give good fits to data, presumably because the calculated gas conductance is too low. For example, Enoeda et al. [7] have fitted their data on several materials using the ZBS model. These fits required contact radii of typically 0.7% of the pebble diameter, which is substantially higher than would be expected from the elastic moduli and the weight of the particle beds. The problem with

obtaining reasonable values for the contact area from these models has also been noted by Xu et al. [8] who obtained acceptable fits for uncompressed beryllium beds using a finite element model with the assumption of point contact only. We are unaware of any analytical model which satisfactorily incorporates the surface roughness between the particles as a measure of the gap width. Moreover, there does not seem to be a clear definition of the roughness height in the literature, and almost no published results include an accurate measurement for particle roughness. A number of analytical models for the conductivity exist which incorporate the gas type and pressure, temperature, and particle size, but all require some adjustable parameters to give acceptable fits to experimental data [9].

The present model has developed out of one by Slavin et al. [10] (henceforth referred to as SLH) that attempted to overcome the above problems. They developed a model for packed spheroids that depended on the small "clam-shaped" gaps that should exist between contacting particles due to undulations in their surfaces. The model used three geometrical parameters of the spheroids: the average spheroid radius R, the average gap radius B, and the average gap width g_{av}. Because these parameters are measurable, in principle, the model held out the hope for calculating the thermal conductivity with no adjustable parameters in cases in which the contact conductance was negligible. When B and g_{av} were used a fitting parameters, this model gave excellent fits [10,11], to the alumina data of SLH [10] in He, the beryllium data of Xu et al. [8] in He and N_2 (henceforth referred to as XAR), and the lithium zirconate [12] data of Earnshaw, Londry and Gierszewski, although in the last case the oblateness of the particles apparently required a third fitting parameter. One of the main conclusions of the SLH paper was that, for the beds studies, the conductance across the particle–particle contact was negligible except under conditions of low gas pressures at low temperature.

An accurately measured value for the roughness of the pebbles used is almost never included in published experimental studies. Therefore, we have measured the surface roughness of the spheroids used in three such studies [7,8,10], to test the validity of the SLH model. It became apparent that the model was not applicable for smooth spheroids such as those of Enoeda et al. [7] (henceforth referred to as EFTKH), for which the spheroids are very smooth with a surface roughness of typically 0.2 μm in height and without undulations of the type needed to create the gaps of the SLH model; rather, for such spheroids, the particle–particle contact is much closer to an ideal point contact than envisaged in the SLH model. Therefore we have modified the original SLH model by replacing the clam-shaped gaps with simple point contacts between two rough spheroids, and reduced the number of required parameters to three—the spheroid radius, the height of the surface roughness and the packing fraction—for the common situation when the thermal conductance between adjacent spheroids by radiation or by the gas is significantly greater than that through the physical point of contact. An operational definition for the height of the roughness has been developed, and a method for determining it, so the model now has no adjustable parameters except when the contact conductance is significant. Having no adjustable parameters is the ultimate goal of the model, since it allows its use for bed design with no experimental data on the conductivity and only measurements on the individual spheroids and the packing fraction.

This revised model is used to compare theoretical values for the bed thermal conductivity for seven sets of experimental data which include pebbles of two different materials, several different sizes and roughnesses, and two different gases. Five of these beds were of alumina spheroids in helium gas: nominally 1- and 3-mm diameter spheroids measured by SLH [10], and 0.3-, 1.0- and 3.0-mm ones measured by EFTKH [7]. The remaining two were of 2-mm Be spheres in helium and nitrogen [8]. Agreement between the theory and experiment is typically within 15%. This should be adequate for many engineering purposes in which pebble compression is not significant. To our knowledge, this is the only model providing this predictive accuracy with no adjustable parameters.

One of the conclusions of this work is that the conduction across the direct contact between spheres did not contribute significantly in the experimental beds addressed in this study. However, for beds in which the particles are compressed together, as in constrained beds of relatively soft materials with substantial thermal expansion, either the assumption of point contacts or the use of the measured roughness height before compression may not be valid. For example, it has been shown that the bed conductivity has a strong dependence on external pressure for beds of aluminum, beryllium, and lithium zirconate particles [13], and a recent paper has shown strong hysteresis in the thermal conductivity due to differential expansion between the bed and its container [14]. Even in such cases the current model should still be useful as the starting point in developing models which do take bed compression into account, since the contact conductance and particle roughness are both included in the model.

2. Theory

It has been shown [15] that, for random packing of spheres, about 73% of nearest-neighbour packing is tetrahedral, with the rest distributed among less-close-packed distributions. The typical packing fraction (fraction of total volume occupied by solid) for such beds is

Table 1
Parameters for the spheroids used in this study

Spheroid type	Average diameter (mm)	Roughness h_r (μm)	Packing fraction (%)
SLH 3 mm alumina	2.70 ± 0.2	1.22 0.71	58
SLH 1 mm alumina	0.94 ± 0.09	1.65 1.53	57.6
EFTKH 3 mm alumina	2.99 ± 0.05	0.22 0.16	65.8
EFTKH 1 mm alumina	1.07 ± 0.03	0.29 0.23	64.9
EFTKH 0.3 mm alumina	0.34 ± 0.02	0.26[a]	58.9
XAR 2.0 mm beryllium	1.80 ± 0.20	1.5	60

[a] Estimated as the value for the 1-mm spheroids.

around 0.57 (see Table 1) although some are as high as 0.65, whereas simple-cubic packing gives 0.54 and close-packing gives 0.74. The deviation from close packing is not surprising for a system in which the spheroids are usually poured en-masse into the receptacle. Many of the particles will fall into the 50% of depression sites which are not those occupied in ideal close packing, thus not only excluding particles from the neighbouring close-packed positions and decreasing the packing density but also causing bridging between spheres to create small regions void of spheres. Therefore, we have modelled the packing as separable into two fractions: one where the spheres are close packed and one where deviations from the close- packed structure has left regions void of any spheres.

The overall unit cell used in the model consists of a close-packed cell in parallel with a void cell. The close-packed cell is shown in Fig. 1. It has area $A_{cp} = 2\sqrt{3}R^2$ perpendicular to the direction of heat flow and height $L = \sqrt{8/3}R$, and contains one particle. The void cell has area A_v and the same height L. The volume of the overall unit cell is $V = A_{cp}L + A_vL$. Knowledge of the packing fraction $p \equiv (4/3)\pi R^3/V$ gives $A_v = [\sqrt{2/3}\pi/p - 2\sqrt{3}] \times R^2$.

The short-range surface roughness, of average height h_r, decreases the gaseous conductivity between contacting spheres by increasing the average gap between them. Therefore, in the close-packed regions, the model treats the spheroids as being perfect spheres, separated at their contact points by a short cylinder of area δ and length $2h_r$. This is shown in Fig. 2, where R is the radius of the spheroid, θ is the polar angle measured from the vertical, and θ_λ is the polar angle for which the separation of the two spheroids is equal to $2/3\lambda$ where the molecular mean free path is λ. (The average distance that a gas molecule travels perpendicular to a surface before colliding with another molecule is $2/3\lambda$ [Ref. [16], p. 264). From (Ref. [17], p. 178) one has

$$\lambda = (\sqrt{2}n\pi D^2)^{-1}, \tag{1}$$

with $n = P/kT$ being the molecular number density, D the molecular diameter, P the gas pressure, T the temperature in kelvins, and k Boltzmann's constant. Both h_r and λ will be assumed to be much less than R except for λ at pressures close to zero. Reference to Fig. 2 gives, for small θ_λ, $\theta_\lambda = (((2/3)\lambda - 2h_r)/R)^{1/2}$ radians and $r_\lambda = (((2/3)\lambda - 2h_r)R)^{1/2}$ for $(2/3)\lambda > 2h_r$, with $\theta_\lambda = 0$ and $r_\lambda = 0$ for $(2/3)\lambda \leqslant 2h_r$.

As sketched in Fig. 2(b), the heat flow will be represented by a number of conductances in series and parallel, including G_s through the solid spheroid, and G_r by radiation between the spheroids. For gaseous conduction, two regions exist between adjacent spheroids: an "inner" region of radius r_λ about the contact point, for which the gap between the two spheroids is less than $(2/3)\lambda$, with a conductance G_i; and an "outer" region for which the gap is greater than $(2/3)\lambda$, with conductance G_o. The conductance through the physical contact of area δ is G_c. Additional conductances must be in-

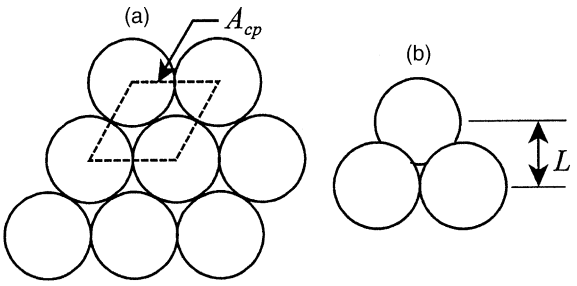

Fig. 1. Unit cell in the close-packed fraction: (a) top view, (b) side view.

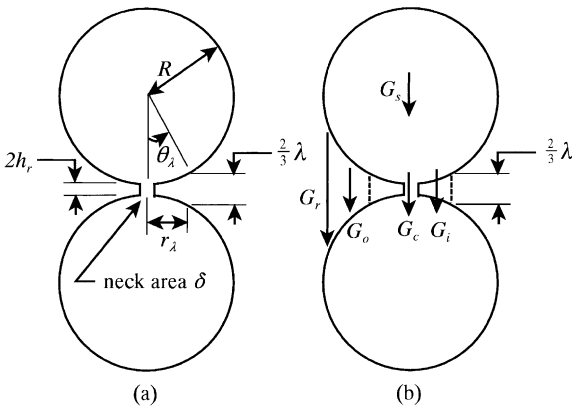

Fig. 2. Model for two contacting spheres: (a) geometrical parameters, (b) conductances.

cluded in the void fraction of the bed: G_{rv} by radiation and G_{gv} by gaseous conduction across the void.

Assuming the physical contact between the two spheroids will be essentially a point contact for hard materials, the conductance G_c through the contact can be ignored as shown previously [10], at least for small, uncompressed experimental beds, except under low gas pressure at low temperature where the radiation and gas conductances are negligible. The expressions for the conductances are the following, with G_o derived later:

$$G_s = \alpha_s K_s \pi R^2/2R, \quad G_c = \alpha_c K_s \delta/2h_r,$$
$$G_r = \alpha_r \frac{4\sigma_s}{2/\epsilon - 1} A_{cp} T^3, \quad G_i = \alpha_i K_i \pi r_\lambda^2/g, \tag{2}$$

$$G_{rv} = \alpha_r \frac{4\sigma_s}{2/\epsilon - 1} A_v T^3,$$
$$G_{gv} = K_o(1 - \exp(-R/\lambda))A_v/L. \tag{3}$$

Here the α's are dimensionless geometrical constants of order unity as discussed below, K_s is the conductivity of the bulk solid material, K_i and K_o are gaseous conductivities as defined later, σ_s is the Stefan–Boltzmann constant, ϵ is the total thermal emissivity (treated as independent of temperature) and g is the average gap between adjacent spheres in the inner region. The radiation conductances both assume a view factor of 1, whereas other expressions also occur in the literature (e.g., [18]). Changing the view factor to that of Ref. [18] would increase the radiative conductance by about 40%; however, the choice of view factor will not make a significant difference in this work since the radiative contribution is small, although it will be important at high temperature. We have assumed the radiation to be isotropic. The exponential term in G_{gv} is a mathematical cut-off to make G_{gv} negligible at low pressures.

If T_1 and T_2 are the temperatures at the top and bottom of the overall unit cell, we can define the effective conductivity over the entire cell in terms of the heat flow $\dot{Q}$ using

$$\dot{Q} = K(A_{cp} + A_v)\frac{T_1 - T_2}{L} = G(T_1 - T_2), \tag{4}$$

where

$$G = G_{cp} + G_v \quad \text{with}$$
$$G_{cp} = \left[G_r + N_c\left(\frac{G_s(G_i + G_o + G_c)}{G_s + G_i + G_o + G_c}\right)\right],$$
$$G_v = (G_{rv} + G_{gv}). \tag{5}$$

Within G_{cp}, G_r is in parallel with the series combination of G_s and $(G_i + G_o + G_c)$. G_{cp} is in parallel with G_v. N_c is the average number of contacts a sphere has per unit cell, in a direction that would allow net heat flow. If the spheres were perfect and close packed, one sphere would contact 12 others. For random packing, the average number of contacts (for packing fractions up to 0.64) is found [19] to be 6. Of these, an average of 3 will be in a plane perpendicular to the direction of heat flow and so will not contribute. Of the remaining 3, 1.5 are in the unit cell of Fig. 1 so $N_c = 1.5$. K_o is the conductivity of the gas (Ref. [17], p.178) in the outer region where $2h_r > 2\lambda/3$, and K_i is the conductivity in the inner region where $2h_r < 2\lambda/3$ (Ref. [17], p. 317), with

$$K_o = \frac{25\pi}{64} n\bar{v}\lambda C_v = \frac{25\pi}{64}\bar{v}\frac{1}{\sqrt{2}\pi D^2} C_v \quad \text{and}$$
$$K_i = \frac{a}{2-a}\frac{\gamma+1}{8} n\bar{v} C_v l. \tag{6}$$

Parameter n is the number of molecules per unit volume, a is the accommodation coefficient and γ is the ratio of the gas heat capacities per molecule, C_p/C_v, where for a monatomic gas $C_p = 5k/2$ and $C_v = 3k/2$, k is Boltzmann's constant, and l is the gap between particles at the point of interest. The average molecular velocity is $\bar{v} = (8kT/\pi m)^{1/2}$ where m is the molecule's mass.

The α parameters of Eqs. (2) and (3) will be discussed using the general expression for thermal conductance G in a material of constant thermal conductivity K,

$$G = \int K\frac{dA}{l} \equiv \alpha K\frac{\pi r^2}{l_o}. \tag{7}$$

Here, dA is the incremental area perpendicular to the direction of heat flow, l is the distance over which the heat is flowing through dA, and πr^2 and l_o are any convenient estimate for, respectively, the total cross-sectional area and average length for the heat flow. For example, for a cylinder of radius r and length l_o with axis parallel to the direction of heat flow, Eq. (7) gives $G = K\pi r^2/l_o$; that is, $\alpha = 1$ in this case. Therefore, the α parameters in Eqs. (2) and (3) can be viewed as geometrical constants of order unity which correct for the fact that the volumes integrated over are not cylinders. For example, if one assumes that the heat flows through a spheroid in straight lines parallel to the cell axis, then it is shown in Ref. [10] that $\alpha_s = 2$. This is greater than1 because the average heat path is much less than $2R$ in length. However, if the heat enters and leaves the spheroid primarily near diametrically opposite points of contact, then α_s will be less than 1 because the average path length is greater than $2R$ and the average cross-sectional area is less than πR^2. As discussed above, for the close-packed fraction of the bed there will be an average of 1.5 heat entry points and 1.5 exit points per sphere, with the minimum distance between contacts being $\sqrt{3}R$, giving an α_s value close to $2/N_c$ per unit cell (with $N_c = 1.5$), the value that will be used in this model. As long as G_s is much greater than the other conductances in the model, the exact value for α_s is not important.

Note that the gap width l cancels in combining Eqs. (6) and (7) in calculating G_i; therefore, no integration is required ($\alpha_i = 1$) and one obtains

$$G_i = \frac{a}{2-a}\frac{\gamma+1}{8} n\bar{v}C_v \pi r_\lambda^2. \tag{8}$$

As pointed out previously [11], the value of r_λ^2 decreases with gas pressure at the same rate as n increases, leaving the value of G_i independent of pressure. For gaseous conduction when the mean free path is less than the gap distance l, the effective gap must be increased (Ref. [17], p. 314) by twice the temperature jump distance $j = ((2-a)/a)(2\gamma/(\gamma+1))(\lambda/Pr)$ where Pr is the Prandtl number; for He, $j = 1.8\lambda$.

Therefore, to obtain G_o using Eqs. (6) and (7), we integrate

$$dA/l = 2\pi R \sin\theta R\cos\theta\, d\theta/(2R - 2R\cos\theta + 2h_r + 2j)$$

over θ from θ_λ to θ_{max}, (the value of $\theta_{max} \sim 60°$ will be discussed below), and multiply by the conductivity K_o to give

$$G_o = K_o \pi R^2 (1 - e^{-R/\lambda})\left\{(\cos\theta_{max} - \cos\theta_\lambda)/R + \frac{R + j + h_r}{R^2}[\ln(R - R\cos\theta_{max} + j + h_r) - \ln(R - R\cos\theta_\lambda + j + h_r)]\right\} \tag{9}$$

This equation is very similar to that given by Schlünder [20], for the gaseous conductance between a particle and the container wall, except that there the integration was carried out from 0° to 90°. Here the exponential term serves the same purpose as for G_{gv}. Normally $R \gg j + h_r$, so the first log term is essentially independent of j and h_r. However, $\cos\theta_\lambda \to 1$ for $2\lambda/3 \sim 2h_r$, so the second log term approaches $\ln(j + h_r)$. Since typically $j + h_r \sim 1 \times 10^{-6}$ m for a 1-mm spheroid, the second log term dominates the first log term and largely determines the value of G_o. This weak logarithmic dependence on $j + h_r$ is an important conclusion of the model.

The question arises as to whether G_o, in Eq. (5), is best treated as being in series or parallel with G_s. The differential value of G_o is proportional to $\sin(\theta)\cos(\theta)/[1 - \cos(\theta) + \tau]$, as discussed above, where $\tau = (h_r + j)/R$. This function is shown in Fig. 3 for various values of τ, while values of λ, θ_λ and τ are given in Table 2 for typical experimental parameters in this study. It is seen from Fig. 3 that the major contribution to G_o occurs for angles <15° from the contact point except at low pressures where λ is large. Therefore, G_o is best treated as being in series with G_s and in parallel with G_i. Finally, in the close-packed fraction one expects the contacts with a given sphere to be separated by about 60°. Therefore, θ_{max} has been chosen to be 60° in Eq. (9), to avoid double-counting of the overlapping G_o contributions, although the difference between using a θ_{max} value of 60° and 90° is small as can be seen from Fig. 3.

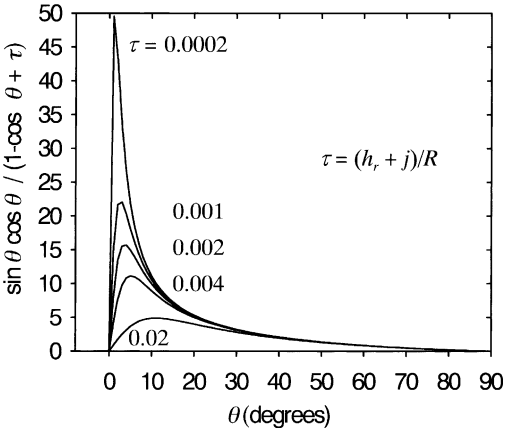

Fig. 3. Plot of $\sin(\theta)\cos(\theta)/(1 - \cos\theta + \tau)$.

Table 2
Values of λ, τ, and θ_λ for typical experimental parameters, for alumina

2R (mm)	P (kPa)	T (K)	h_r (μm)	λ (μm)	τ	θ_λ (°)
1	100	300	0.15	0.2	0.001	0
1	100	800	0.15	0.53	0.002	1.2
1	5	300	1.5	4	0.017	2.6
0.3	100	300	0.2	0.2	0.001	0

3. Experimental determination of the value of h_r

The surface roughness of the spheroids has been measured using a Talyrond stylus profilometer (model 100, Taylor–Hobson, USA), with a radial resolution of about 0.2 μm. However, the tips supplied with the profilometer were too blunt to provide the roughly 1-μm lateral resolution required. Consequently, tips were fabricated using tungsten wire of 0.25-mm diameter and the NaOH-etch technique commonly used to prepare tips for scanning tunnelling microscopy [21]. Tungsten has the advantage of being very hard, so the tips do not abrade as rapidly as other metals on the ceramic spheroids. The tips had an end radius of about 1 μm, as determined by optical microscopy. Even with tungsten, it is difficult to maintain a tip radius of 1 μm, because of the hardness of the ceramic and the tip-surface pressure required by the profilometer. An instrument similar to an atomic force microscope (AFM), which operates with either zero or very low contact force, would be preferable but conventional AFMs do not have the required

horizontal range. Measurements with an AFM on some of the spheres yielded values for h_r similar to those from the Talyrond traces; however, the AFM scans were done over a lateral distance of only 10–60 μm, and so did not provide as good an average for the roughness as the Talyrond traces.

To measure the roughness, a spheroid was glued to the end of a spindle mounted in a holder centred on the revolving disk of the profilometer. The profilometer produces a spark trace on a paper disk, which can be calibrated against a protrusion of known height. The spark trace was scanned into a computer and extraneous markings removed manually. The resulting figure will henceforth be called the "spheroid profile". An IDL (Research Systems, Inc.) program [22] was written to determine the centroid of the sphere profile, and the local distance $R(\theta)$ of every point from the centroid was then calculated.

Usually spheroids in packed beds are poured into the container until it is full before any vibration is applied. Therefore, the spheroids will not normally rotate more than a few degrees about the initial point of contact before being trapped in position by adjacent spheres, unlike the assumptions of the SLH model which would require substantial rotations for the spheroids to reach equilibrium positions. The assumption of a limited rotation leads to the following method for calculating the surface roughness h_r from the spheroid profile.

It is impossible to estimate how the peaks and valleys on two rough spheroids will intermesh on contact, so we considered the contact of a smooth sphere with an irregular one of the same radius represented by the measured spheroid profile as sketched in Fig. 4. The spheroids considered in this paper have peak-to-peak roughness of order 1 μm over a distance of several microns, but radii of order 1 mm, so the true curvature of the spheres will be much less than shown in Fig. 4. These two "circles" were brought together along a line through their centres in the IDL program, until contact was made at some initial point P_1. Treating the smooth sphere as the one which was dropped, we then started a computer search for a nearby point (P_2) which was the local extremum (more precisely, the point for which the angle ω was maximum) against which the smooth sphere would come to rest. This search was limited to the physically significant region between P_1 and the point P_3,

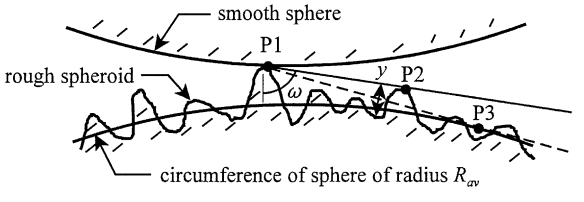

Fig. 4. Method for determining roughness h_r.

the latter being the contact of the tangent drawn from P_1 to the circle of measured average radius R_{av} centred on the centroid of the rough sphere. The separation of the two spheres at any point is the height of the perpendicular y dropped from the line P_1P_2 to the rough sphere. (The circumference of the smooth sphere essentially coincides with the line P_1P_2, because $R \gg h_r$.) The average value y_{av} of y was then calculated between P_1 and P_2. This procedure was repeated using P_2 as the "initial" point of contact, and so on around the entire profile of the rough spheroid. The average value of y_{av} over the entire circumference was used as the value for h_r in the model. Of course, the contacting spheres in three dimensions will settle to a third contact point, but this will not change the value of h_r significantly, given its logarithmic dependence in Eq. (9).

If the radius of the profilometer tip is larger than the distance between surface peaks, then the value calculated for h_r will be too small. The value of λ is 0.2 μm for He gas at 300 K and 1 atmosphere pressure so, from Eq. (9), the value of h_r must be substantially smaller than 0.2 μm before it can be ignored under these conditions. Therefore, one must take care that the profilometer is providing an accurate value for h_r by taking more than one measurement with different tips. Measured values for h_r for two spheres from each experimental set are given in Table 1, except for the Be spheres for which only one sphere was measured. The 0.3-mm diameter sphere from EFTKH was too small to mount reliably on the profilometer, so its roughness has been estimated as the same as for the 1-mm diameter spheres.

4. Comparison of theory and experiment

In all the plots of thermal conductivity as function of temperature given below, the points are the experimental data and the lines represent the calculations using the values of h_r in Table 1, using a SigmaPlot 4.0 program [22]. The theory is compared to seven sets of experimental data. In all cases, a value of 1 has been used for the accommodation coefficient a in the expression for G_i, and a value of $\alpha_r = 1$ in the radiation terms, as discussed previously [10]. However, the exact value of these two parameters turns out to be largely immaterial because the magnitudes of G_i, G_r and G_{rv} are much smaller than that of G_o for the cases considered. As stated earlier, the value of $\alpha_s = 2/N_c$ was used in the calculations. Again, the exact value for α_s turns out not to be critical because the value of $G_i + G_o + G_c$ is many times less than G_s, with which it is in series, so G_s typically has $<10\%$ effect on the conductivity which is dominated by G_o. This explains why experimental results with pebbles of very different materials usually produce similar values for the same gas. Finally, the value of G_c has been taken to be negligible under the assumption of point contacts for

alumina, as has previously been shown to be appropriate [10], but in the case of beryllium it has been determined from the measured thermal conductivity at $P = 0$ kPa. For illustrative purposes, the relative sizes of the G values as a function of temperature can be seen in Fig. 5 for the 3-mm SLH spheres for $P = 4.8$ kPa. The values in Fig. 5 have been scaled as indicated, so they can all be compared on one plot. It is seen that, in this case, G_o dominates the conductivity (since G_s is in series with G_o), and therefore continues to dominate at gas pressures above 4.8 kPa. This was true for all the alumina beds studied.

4.1. Slavin et al. data

In this study [10], rough alumina spheres of nominally 3- and 1-mm diameter were used; the experimental results are compared with theory in Figs. 6 and 7, respectively, over temperatures from about 350 to 800 K, and gas pressures from 0 to 100 kPa, using the particle roughness measured by us. For the calculations, K_s was represented by quadratic expressions [10] fitted to the thermal conductivities provided by the supplier. For the $P = 0$ kPa curves, the theoretical curve uses only the radiation term of Eq. (2). Calculated values for G_r, G_o, G_i, G_s, G_{rv} and G_{gv} for the 1-mm spheroids at 100 kPa and 650 K are, respectively, 2.8×10^{-5}, 1.4×10^{-3}, 0, 1.4×10^{-2}, 8.7×10^{-6} and 6.8×10^{-5} $\mathrm{W\,s^{-1}\,K^{-1}}$. The zero value for G_i occurs because $2\lambda/3 < 2h_r$ under these conditions.

The theory accounts well for the dependence on temperature, pressure, and particle size and roughness, with agreement with experiment generally better than 15%. Apart from the zero-pressure curve at high temperature for the 3-mm spheroids, the worst percentage agreement is for pressures near 4 kPa. As discussed earlier, the assumption that G_o can be treated in series with G_s was based on the observation that most of the heat transfer via G_o occurs within about 15° of the contact points. As can be seen from Fig. 3 and Table 2, this assumption is least justified at low pressures, and reducing the magnitude of G_o in series would improve the agreement near 4 kPa.

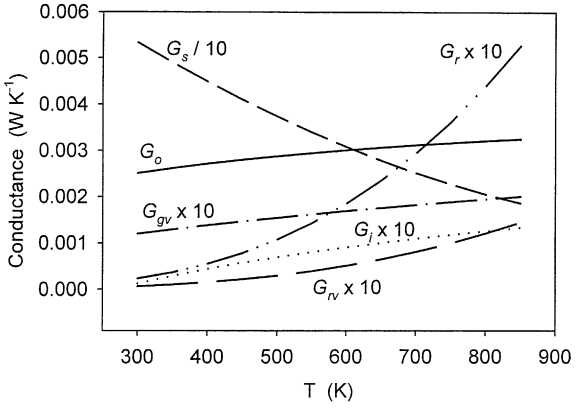

Fig. 5. Values of conductances for the 3-mm SLH alumina spheroids, at 4.8 kPa.

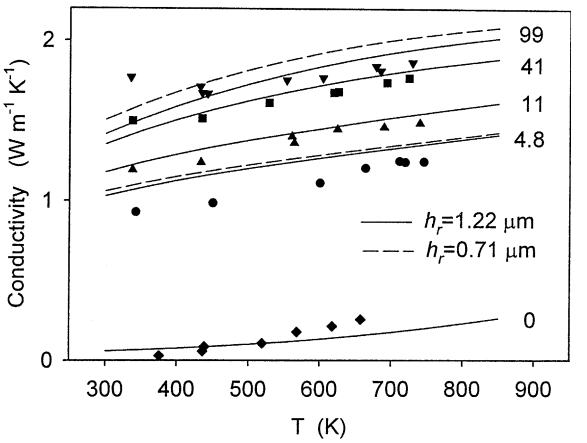

Fig. 6. Thermal conductivity for the 3-mm SLH alumina spheroids. Points are experimental data; lines are from the present theory. The pressures in kPa are given at the right.

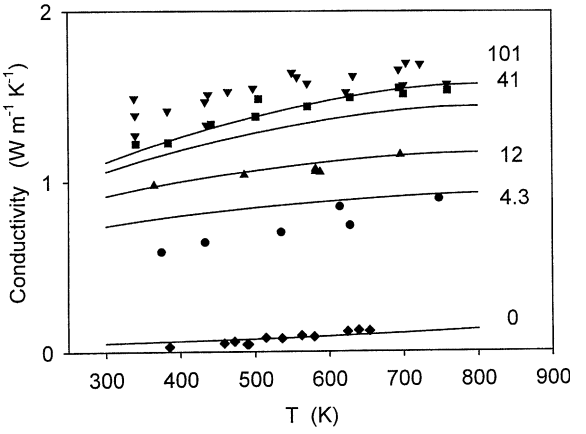

Fig. 7. Thermal conductivity for the 1-mm SLH alumina spheroids. Points are experimental data; lines are from the present theory. The pressures in kPa are given at the right.

4.2. Enoeda et al. data

This work used quite smooth alumina spheres of nominally 3-, 1- and 0.3-mm diameter [7]; samples of the spheroids were generously provided by Dr. Enoeda for our measurement of the roughness. The thermal conductivity of the solid material was unknown, but since it was claimed to be dense alumina the best published data

[23] for this material have been used. Over the temperature range of interest, that data for K_s fits well to the expression $43.4 - 0.0656T + 2.93^{-5}T^3$ W m^{-1} K^{-1}. The solid lines in Fig. 8 compare theory with the experimental results as a function of T at 100 kPa pressure, using these K_s values. The theory accounts well for changes in the particle size and pressure. Calculated values for G_r, G_o, G_i, G_s, G_{rv} and G_{gv} are (for the 3-mm diameter spheres), respectively, 2.9×10^{-4}, 6.5×10^{-3}, 0, 5.0×10^{-2}, 3.6×10^{-5} and 8.8×10^{-5} W s^{-1} K^{-1} at 100 kPa and 650 K. For comparison, the dashed lines in Fig. 8 used the values of K_s for the 3-mm SLH spheres, and provide significantly better agreement with experimental data. This emphasizes the need for accurate values of K_s even given that G_o dominates the conductivity.

4.3. Xu et al. data

Finally, the dependence of the theory on the gas employed was checked against experimental data by Xu et al. [8] on nominally 2-mm diameter beryllium spheroids using both He and N_2 gases at an average temperature of 308 K, and the values for the gas parameters given previously [10]. Dr. Abdou has generously sent us samples of those spheroids for measuring the roughness. Theory (lines) and experiment (points) are compared in Fig. 9. The temperature was so low that the conduction through the point of contact dominated the zero-pressure results, so the value for G_c had to be obtained from the experimental value $K(0)$ of the conductivity at zero pressure using $G_c = K(0)(A_{cp} + A_v)/(N_c L)$. The values of $K(0)$ in Ref. [8] ranged from about 0.45 to 0.55 W m^{-1} K^{-1} whereas the theoretical results in Fig. 9 required a value of 0.35 for best agreement with experiment. Increasing this to 0.45 increases the theoretical value of the thermal conductivity by 0.1 W m^{-1} K^{-1} and worsens agreement by only this amount. The conductivity of Be was assumed to be constant over the small temperature range used (30–40 °C) and taken as $K_s =$ 200 W m^{-1} K^{-1} [24]. However, this is such a large value that changing it by 10% made no significant difference to the conductivity. The theory accounts well for both the change in gas from He to N_2, and the dependence on gas pressure. The present theory fits the experimental data better than any of the any of the models considered by Xu et al. [8], including a finite element calculation.

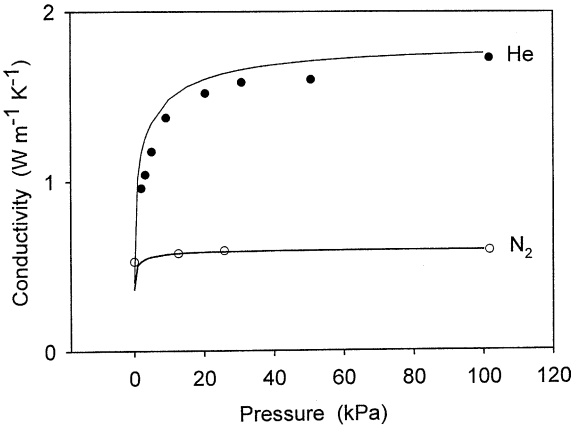

Fig. 9. Thermal conductivity for the XAR beryllium spheroids. Points are experimental data; lines are from the present theory.

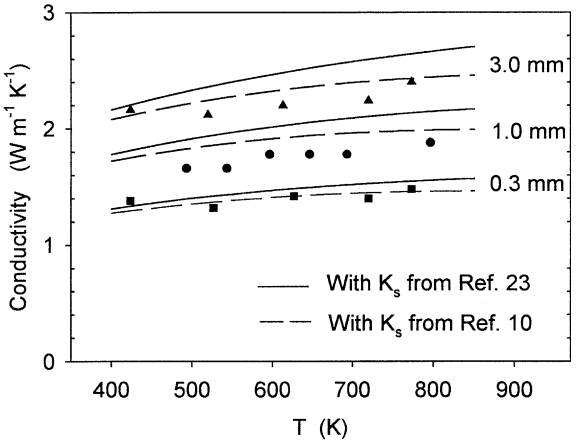

Fig. 8. Thermal conductivity for the EFTKH alumina spheroids. Points are experimental data; lines are from the present theory. Nominal sphere diameters in mm are at the right.

5. Discussion

The theory agrees with the experimental data within about 15%. It is successful in predicting the dependence on bed conductivity of the particle diameter (Fig. 8, and Fig. 6 vs. Fig. 7), type of gas (Fig. 9), and gas pressure (Figs. 6, 7, and 9). It also shows clearly the importance of surface roughness on bed conductivity: the conduction is significantly higher for the smoother alumina spheroids (EFTKH, Fig. 8) than the rough ones (SLH, Figs. 6 and 7) for particles of the same material and diameter. Unfortunately, published results rarely, if ever, have included an accurate measurement of particle roughness, which prevents a comparison of the present theory with more published experimental data. The model also provides a good fit to experimental data without the need to assume an unrealistically high contact area between particles.

Although the agreement between experiment and theory was marginally better with the SLH model [10], the present model is clearly much superior because the SLH model uses two adjustable parameters whereas the current model requires none except at low temperature

at low gas pressures where the contact conductance must become dominant and will need to be fitted in any model, including the SLH model.

A strong point of the current model is the ability to compare the individual conductances calculated, as in Fig. 5, in order to check the assumptions of the model for a given pebble bed. For example, it is clear for the beds considered that the conductance G_o through the gas near the points of contact is the dominant contribution except for Be near zero gas pressure or when N_2 is used.

One of the driving forces behind the SLH model was the attempt to include the transition in the thermal conductivity from a linear dependence on pressure at low pressures to independence of pressure at high pressure, as shown in Fig. 9. This transition must occur as the gas mean free path changes from being less than some critical length of the system to being greater than this length, and led to the inclusion of this critical length as the gap width between particles. From Eq. (6) we know that the conductivity at low pressure increases linearly with pressure. Therefore, the pressure (about 5 kPa) at which the initial linear portion in Fig. 9 reaches the value for high pressure should give approximately the value of the mean free path as equal to $2h_r$, using Eq. (1). This gives $h_r \sim 2$ μm for both gases in Fig. 9, and about the same value when this analysis is done for the 1-mm SLH spheres. These compare well to average h_r values in Table 1, measured with the profilometer, of 1.6 and 1.5 μm, respectively.

The model presented here is in process of being extended to the case of beds containing two particle sizes with one small enough that they flow between the interstices of the other.

6. Conclusions

A revised analytical model with no adjustable parameters has been developed for the thermal conductivity of uncompressed, packed beds of spheroidal pebbles in the presence of a static gas, provided the conductivity of the solid material is much greater than that of the gas, and the conductance through the direct contact between particles is negligible relative to that of either radiation or the gas. The main innovations of the current theory are the following:

(a) The model includes the particle roughness explicitly. This is an essential parameter in that it determines the average separation of the particles, which in turn controls the gaseous contribution to the conductivity. It is shown that this contribution depends logarithmically on the local roughness of the pebble surface. Therefore it is crucial that the measured roughness be included in all future experimental studies of bed thermal conductivity to allow theoretical modelling.
(b) An operational definition of the roughness and a procedure for measuring it are provided.
(c) The model uses the bed packing fraction to separate the bed into a close-packed fraction and a void fraction, which have to be treated differently.
(d) It uses results from the literature to define the average number of contacts per particle. This is important because, for all but one of the experimental test beds considered, it is the gas near the point contacts that contributes most to the conductivity.
(e) The clear analytical separation of the main conductances contributing to the overall conductivity allows one to determine the contribution of each. This should help in the design of a bed for a specific purpose.

The model has been tested against seven sets of experimental data involving two different gases and solids, different particle sizes and roughness, and over a wide range of pressure and temperature, with results that agree with experiment within about 15%. In the experimental cases considered, the temperatures were low enough that radiation was not a major contributor to the conduction, so it is desirable to test the model at higher temperatures than done here. It is noted that a value for the contact conductance will be required for any model at low pressure and temperature where the gaseous and/or radiative conductivity do not dominate the conductivity, and the value measured for the roughness of uncompressed pebbles may not be an appropriate measure of the pebble separation if the pebbles are compressed. However, this model should serve as a useful starting point for developing models for such beds.

Acknowledgements

The authors wish to acknowledge the financial support of the Natural Sciences and Engineering Research Council of Canada for this research and for a Summer Undergraduate Research Award for CG. Appreciation is expressed to J. Hutter for the AFM measurements, and to A. DeMonte and Fleming College for the loan of the profilometer.

References

[1] F.A. Londry, A.J. Slavin, Thermal conductivity of a packed bed of hollow zirconia microspheres, under vacuum and under 100 kPa of argon, J. Am. Ceramic Soc. 74 (1991) 3118–3125.
[2] D.L. McElroy, D.W. Yarbrough, G.L. Copeland, F.J. Weaver, R.S. Graves, T.W. Tong, H.A. Fine, Development

of advanced thermal insulation for appliances, Oak Ridge National Laboratory Report ORNL/CON-159, 1984.
[3] J.D. Sullivan, C.L. Brayman, R.A. Verrall, J.M. Miller, P.J. Gierszewski, F. Londry, A. Slavin, Canadian ceramic breeder sphere-pac technology: capability and recent results, Fusion Eng. Des. 17 (1991) 79–95.
[4] M.G. Freiwald, W.R. Paterson, Accuracy of model predictions and reliability of experimental data for heat transfer in packed beds, Chem. Eng. Sci. 47 (1992) 1545–1560.
[5] D.U. Ringer, Heat transfer across small gaps, in: S. Mujumdar (Ed.), Drying of Solids, Wiley and Sons (Halstead Press), New York, 1986, pp. 84–90.
[6] R. Bauer, E.U. Schlünder, Effective radial thermal conductivity of packings in gas flow. Part II. Thermal conductivity of the packing fraction without gas flow, Int. Chem. Eng. 18 (1978) 189–204.
[7] M. Enoeda, K. Furuya, H. Takatsu, S. Kikuchi, T. Hatano, Effective radial thermal conductivity measurements of the binary pebble beds by hot wire method for the breeding blanket, Fusion Technol. 34 (1998) 877–881.
[8] M. Xu, M.A. Abdou, A.R. Raffray, Thermal conductivity of a beryllium gas packed bed, Fusion Eng. Des. 27 (1995) 240–246.
[9] E. Tsotsas, H. Martin, Thermal Conductivity of packed beds: a review, Chem. Eng. Process. 22 (1987) 19–37.
[10] A.J. Slavin, F.A. Londry, J. Harrison, A new model for the effective thermal conductivity of packed beds of solid spheroids: alumina in helium between100 and 500 °C, Int. J. Heat and Mass Transfer. 43 (2000) 2059–2073.
[11] A.J. Slavin, Test of a new model for the effective thermal conductivity of a packed bed in gas: lithium zirconate spheres in helium, Fusion Eng. Des. 54 (2001) 87–95.
[12] J.W. Earnshaw, F.A. Londry, P.J. Gierszewski, The effective thermal conductivity of a bed of 1.2-mm diam lithium zirconate spheres in helium, Fusion Technol. 33 (1998) 31.
[13] F. Tehranian, M.A. Abdou, M.S. Tillack, Effect of external pressure on particle bed effective thermal conductivity, J. Nuc. Mater. 212–215 (1994) 885–890.
[14] M.D. Donne, A. Goraieb, G. Piazza, F. Scaffidi-Argentina, Experimental investigations on the thermal and mechanical behaviour of single size beryllium pebble beds, Fusion Technol. 38 (2000) 290–298.
[15] J.L. Finney, Local structure of disordered hard sphere packings, in: D. Bideau, A. Hansen (Eds.), Disorder and Granular Media, North-Holland, Amsterdam, 1993, pp. 35–54.
[16] F.W. Sears, An Introduction to Thermodynamics, the Kinetic Theory of Gases, and Statistical Mechanics, second ed., Addison-Wesley, Reading, MA, 1952.
[17] E.H. Kennard, Kinetic Theory of Gases, McGraw-Hill, New York, 1938.
[18] N. Wakao, K. Kato, N. Furuya, View factor between two hemispheres in contact and radiation heat-transfer coefficient in packed beds, Int. J. Heat and Mass Transfer 12 (1969) 118–120.
[19] J.P. Troadec, J.A. Dodds, Global geometrical description of homogeneous hard sphere packings, in: D. Bideau, A. Hansen (Eds.), Disorder and Granular Media, North-Holland, Amsterdam, 1993, pp. 133–163.
[20] E.U. Schlünder, Particle heat transfer, in: Heat Transfer 1982, Proc. 7th Int. Heat Transfer Conference, München, 1982, pp. 195–211.
[21] J. Chen, in: Introduction to Scanning Tunneling Microscopy, Oxford University Press, Oxford, 1993, p. 283.
[22] The IDL and SigmaPlot programs used in this work can be found at www.trentu.ca/academic/physics/aslavin.
[23] W.D. Kingery, Thermal conductivity: VI, Determination of conductivity of Al_2O_3 by spherical envelope and cylinder methods, J. Am. Ceramic Soc. 37 (1954) 88–90.
[24] D.W. Gray (Ed.), American Institute of Physics Handbook, second ed., McGraw-Hill, New York, 1963.